Superconductivity in the hexagonal-layered molybdenum carbide η-Mo$_3$C$_2$

K. Yamaura,[1,*] Q. Huang,[2] M. Akaishi,[1] and E. Takayama-Muromachi[1]

[1]*Advanced Nano Materials Laboratory, National Institute for Materials Science, 1-1 Namiki, Tsukuba, Ibaraki 305-0044, Japan*
[2]*NIST Center for Neutron Research, National Institute of Standards and Technology, Gaithersburg, Maryland 20899, USA*
(Received 8 July 2006; revised manuscript received 7 September 2006; published 8 November 2006)

The hexagonal-layered superconductor η-Mo$_3$C$_2$ (T_c=8.5 K) was investigated by neutron diffraction, magnetic susceptibility, and specific-heat measurements. A significant layered character was found in the structure, which comprises edge-sharing CMo$_6$ octahedra sheets and ~50% carbon occupied blocks. Magnetic characterization revealed the Ginzburg-Landau parameter of η-Mo$_3$C$_2$ is ~26, which is close to that for the comparable T_c compound Li$_2$Pd$_3$B (~21), but less than a half of that for MgCNi$_3$ (~54). The molybdenum carbide would provide valuable opportunities to deepen understanding of those unconventional superconductors.

I. INTRODUCTION

Nonoxide superconductors have been attracting renewed interest because those superconducting properties are remarkable, such as the relatively higher critical temperature (T_c) of MgB$_2$ (Ref. 1) and unusual interplay between magnetism and electronic correlations in $LnTr_2$B$_2$C.[2–4] Another nonoxide superconductor, even if T_c is lower than that of HTSC, would probably hold considerable scientific value as well as practical worth.

The nonoxide perovskite MgCNi$_3$ recently attracted much attention as the superconductivity at 8 K was confirmed instead of an expected itinerant ferromagnetism.[5] We then focused our efforts on the transition-metal carbides in search of valuable superconducting materials. First, we surveyed the Mo-C chemical system because the highest T_c was reported in binary carbides; the T_c for the cubic δ-MoC$_{1-x}$ was 14.7 K, and 9 K for the hexagonal η-Mo$_3$C$_2$.[6–12] However, the nature of the superconductivity has not been verified, probably because the superconductivity was complicated somewhat by their own chemical problems, including carbon nonstoichiometry and thermodynamical structure instability, which were sensitive to the synthesis above 2000 °C.[6–12]

We thus applied a high-pressure method to the synthesis and a clear improvement of sample quality was achieved for η-Mo$_3$C$_2$. The sample allowed us to conduct a systematic investigation on the superconductivity by means of neutron diffraction and magnetic characterizations, while the synthesis effort to prepare a high-quality sample of the cubic δ-MoC$_{1-x}$ was continued.

The superconducting phenomenological parameters of η-Mo$_3$C$_2$—including the lower and the upper critical magnetic fields, the magnetic penetration depth, and the coherence length—were determined in this study, and the neutron structure data revealed that the hexagonal η-Mo$_3$C$_2$ holds a significant layered character, indicating a possibility of anisotropic superconductivity.

II. EXPERIMENTAL

Polycrystalline samples with nominal compositions Mo$_3$C$_{2-\delta}$ at δ=0.0, 0.1, and 0.2 were prepared from fine Mo powder (99.99%, ~3 μm) and carbon powder (Tokai Car-bon). The starting powders were mixed and each set in Ta capsule with h-BN inside, which prevents direct contact with the Ta capsule of the mixture. The capsules were set in a high-pressure furnace capable of maintaining 6 GPa during heating, and heated at 1700 °C for 1 h. After the heating, the capsule was quenched in the furnace before releasing the pressure.

The crystal structure of the superconducting phase (T_c=7.4 K, determined by a specific heat study, shown later) was studied by a neutron diffraction method (Fig. 1). The sample powder was set in the BT-1 high-resolution diffractometer at the NIST Center for Neutron Research. A Cu(311) monochromator with a 90° takeoff angle, λ=1.5403(2) Å, and in-pile collimation of 15 min of arc were used. Data were collected over the 2θ range between 3° and 168° with a step of 0.05°. A Ge(311) monochromator, λ=2.0787(2) Å, was also used instead of the Cu(311) monochromator. Detailed description for the neutron instrument is available online.[13] The sample was at room temperature during the measurement. Neutron scattering amplitudes used in data refinements were 0.665 and 0.672 (10^{-12} cm) for C and Mo, respectively.

A part of the sample as made was wired for a four-terminal method to measure the electrical resistivity. The study was conducted between 2 K and 300 K in a commercial apparatus [Quantum Design, Physical Properties Measurement System (PPMS)]. The ac-gage current was 30 mA and the ac frequency was 30 Hz. Specific heat of the sample was measured in the PPMS apparatus by a time-relaxation method between 1.8 K and 9 K. Magnetic susceptibility was measured in a magnetic field of 50 Oe; the sample was cooled down to 2 K without the field, and then the magnetic field was applied, followed by heating to 10 K (zero-field cooling, ZFC) and cooled down again to 2 K (field cooling, FC) in a commercial apparatus [Quantum Design, Magnetic Property Measurement System (MPMS)]. The magnetization to ±50 kOe was measured in MPMS at 1.8 K.

III. RESULTS AND DISCUSSION

The structure refinement analysis was conducted on the neutron diffraction pattern with the software GSAS.[14,15] The pattern taken at λ=1.5403 Å was tested at first with a two-
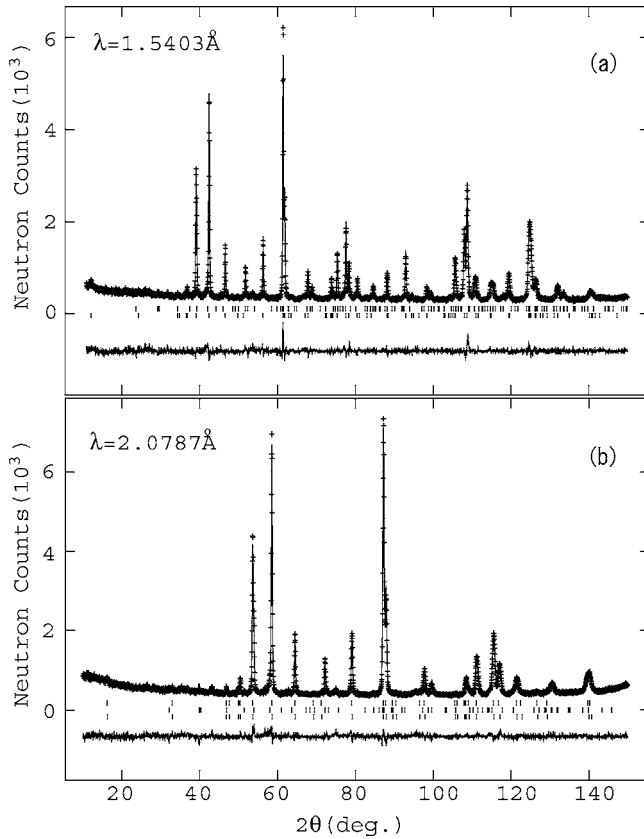
FIG. 1. Powder neutron diffraction profiles of the sample at the nominal composition $Mo_3C_{1.8}$, taken at $\lambda = 1.5403$ Å (a) and 2.0787 Å (b). Observed (crosses) and calculated (solid lines) intensities and the difference between those (bottom) are each shown. Vertical small bars indicate calculated reflection positions for η-Mo_3C_2 [(a) upper; (b) upper], α-Mo_2C [(a) lower; (b) center], and another η-Mo_3C_2 that has slightly different carbon content and lattice parameters [(b) lower]. The measurements were conducted at room temperature.

phase mode for η-Mo_3C_2 and α-Mo_2C.[6–12] As shown in Fig. 1(a), the fitting quality seemed fair ($R_{wp} = 6.37\%$, $R_p = 4.90\%$, and $\chi^2 = 2.226$), but we believed there should be a way to reach a much better quality. We considered a possibility of local segregation in η-Mo_3C_2 due to an inhomogeneity of carbon distribution. We thus tested two hexagonal phases simultaneously, which were assumed to share the same structure basis (η-Mo_3C_2) but have slightly different carbon content and lattice parameters.

In order to test the possibility of the small structure disagreement in a more reliable way, we increased the peak resolution by switching the monochromator from Cu(311) to Ge(311). We succeeded in obtaining a diffraction pattern at $\lambda = 2.0787$ Å for the same sample. Obviously, analysis on this newer pattern was the result of a clear improvement of fitting quality; the best achievement is shown in Fig. 1(b) ($R_{wp} = 6.18\%$, $R_p = 4.78\%$, and $\chi^2 = 2.099$), and the structure solutions are listed in Table I. The results indicate that the superconducting hexagonal Mo_3C_2 phase is carbon nonstoichiometric, and it is possible to find at least two different carbon compositions (formula sum: $Mo_6C_{3.564}$ and $Mo_6C_{3.926}$). Their weight fractions were respectively 0.48 and 0.39, while the remaining 0.13 is due to α-Mo_2C, which was probably produced by decomposition of η-Mo_3C_2 in the quench process, as reported elsewhere.[11]

The schematic structure view is shown in Fig. 2, which is based on the current results. The most remarkable point we found is a layered feature produced by partial carbon occupancy ($\sim 50\%$) at the C2 site. The structure of the superconducting η-Mo_3C_2 could be characterized as an alternate stacking of the edge-sharing C1-Mo_6 octahedra sheet (the bottom of Fig. 2) and the nearly 50% carbon occupied C2-Mo_6 double-layers block (the top of Fig. 2). As the CNi_6 octahedra network was found crucial to produce the superconductivity in $MgCNi_3$,[5] the hexagonal CMo_6 sheet is expected to play a significant role in the superconductivity in η-Mo_3C_2.

TABLE I. Atomic coordinates and isotropic displacement parameters of the superconducting η-$Mo_3C_{2-\delta}$. (top) formula sum $Mo_6C_{3.564}$,[a] and (bottom) formula sum $Mo_6C_{3.926}$.[b]

Atom	Wyckoff Position	x	y	z	$100U_{iso}$ (Å^2)	Fraction
Mo1	2b	0	0	1/4	0.56(4)	1
Mo2	4f	1/3	2/3	0.08553(8)	0.42(3)	1
C1	2a	0	0	0	0.79(7)	0.828(20)
C2	4f	1/3	2/3	0.67142(14)	0.28(9)	0.477(14)
Mo1	2b	0	0	1/4	0.56(4)	1
Mo2	4f	1/3	2/3	0.08619(8)	0.42(3)	1
C1	2a	0	0	0	0.79(7)	0.935(23)
C2	4f	1/3	2/3	0.67093(14)	0.28(9)	0.514(13)

[a]Space group: $P6_3/mmc$, $a = 3.01050(13)$ Å, $c = 14.6112(6)$ Å, Cell volume = 114.681(11) Å^3, $d_{cal} = 8.955$ g/cm^3. The weight fraction was 0.4809(18).
[b]Space group: $P6_3/mmc$, $a = 3.01313(14)$ Å, $c = 14.6372(6)$ Å, Cell volume = 115.086(12) Å^3, $d_{cal} = 8.986$ g/cm^3. The weight fraction was 0.38954(95).
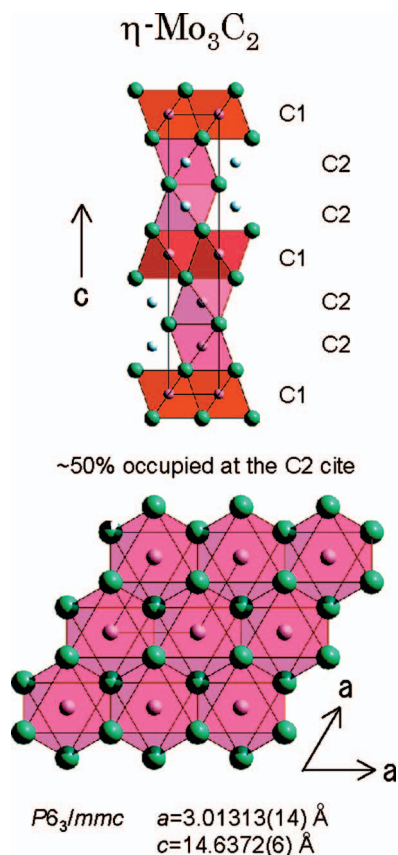
FIG. 2. (Color) Schematic structure view of η-Mo_3C_2, drawn with the neutron diffraction results. The CMo_6 octahedra were enhanced in color.

The magnetic characterization of the superconducting transitions is shown in Fig. 3(a) and 3(b). The magnetic onset of the superconductivity ranges from 8.5 K (for the nominal carbon content of 1.9 per the formula mole) to 7.8 K (for the 1.8 per the mole). The superconducting volume fraction of the loose powder sample was $\sim$100% for the ZFC data and $\sim$16% for the FC data at 2 K (for $Mo_3C_{1.8}$), confirming that the η-Mo_3C_2 phase is exactly superconducting at $\sim$8 K rather than at other phases, such as the impurity α-Mo_2C. The carbon content 3.0 was tested under the same synthesis condition and the transition was observed at 8.5 K; however, the superconducting volume fraction was remarkably reduced ($<$50%, ZFC). The observation indicates that the composition of 3.0 is clearly out of the chemical range of the structure. The small variation of the superconducting transition temperature probably reflects the variable carbon concentration in the η-Mo_3C_2 structure. Within our study, the highest T_c was 8.5 K (magnetic characterization).

Additional magnetic characterization was conducted at 1.8 K. A magnetic hysteresis loop was measured in a field cycle between 55 kOe and $-$55 kOe. The central part of the M versus H loop was expanded and shown in the main panel of Fig. 3(b). The observed character is a typical of the type-II superconductor, and the lower critical field was estimated $\sim$130 Oe, as a minimum point of the curve. The magnetic irreversibility field (H_{irr}) was also determined to be $\sim$40 kOe with a criterion of 1 (10^{-3} emu/g), as shown in the inset of Fig. 3(b).
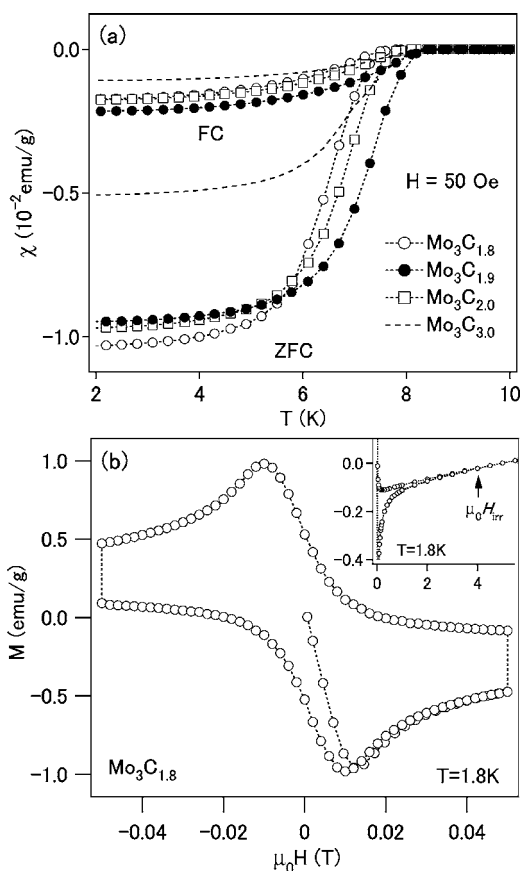
FIG. 3. Magnetic characterization of the superconducting transitions for the molybdenum carbide of nominal composition $Mo_3C_{3-\delta}$. (a) Data taken on heating after cooling in the absence of a field (zero-field cooling, ZFC), and on cooling (field cooling, FC) in an applied field of 50 Oe. (b) Magnetization curve at 1.8 K measured in a loop between 50 kOe and $-$50 kOe. All samples were in a form of loose powders. The irreversibility point is indicated by an arrow in the inset.

Temperature dependence of the electrical resistivity of η-Mo_3C_2 (nominal composition $Mo_3C_{1.8}$) between 2 K and 300 K is shown in Fig. 4. The normal-state resistivity is fairly low ($\sim$0.11 mΩ cm at room temperature), although it is of the polycrystalline form. However, the ratio ($\rho_{300 K}/\rho_{9 K}$) is poor, indicating a possibility of substantial influence of impurities on the charge transport. Further studies using a single crystal, if it is available, would be significant to verify the possibility. The T_c onset is 7.9 K and the transition width (10%/90%) is $\sim$0.2 K.

The magnetic field-dependent resistivity was measured for the same sample between 2 K and 9 K. The data are shown in the inset of Fig. 4. The superconducting transition temperature goes down with increasing magnitude of the field, being consistent with a conventional superconducting picture.[16] The superconductivity completely disappeared in the field of 90 kOe above 2 K. The upper critical field of η-Mo_3C_2 determined by the electrical measurements is discussed later.

The characterization of the superconducting transition by specific heat measurement is shown in Fig. 5. The main panel shows field dependence of the superconducting transi-
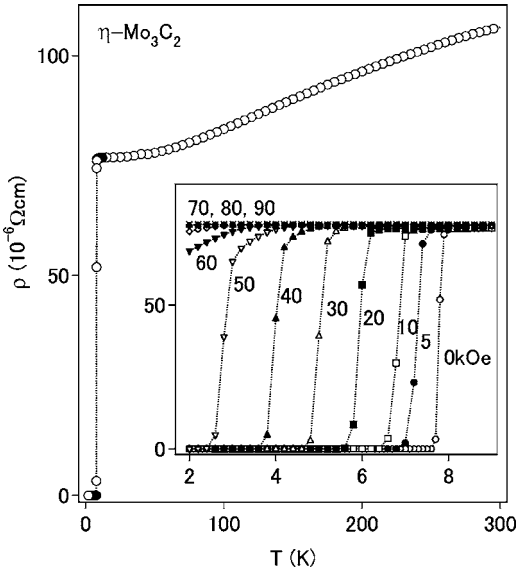
FIG. 4. Temperature dependence of the electrical resistivity of η-Mo$_3$C$_2$ (nominal composition Mo$_3$C$_{1.8}$). (Inset) Characterization of the superconducting transition under a variety of magnetic field.

tion in the C$_p$/T versus T^2 plots. At 70 kOe the superconducting transition is perfectly suppressed and hence the data provide us an extrapolation of the normal-state behavior to the $T=0$ limit, which corresponds to the Sommerfeld constant (γ) of the Fermi-liquid term $C(T)/T = \gamma + \beta T^2$, where β denotes a lattice contribution coefficient. We obtained $\gamma = 11.8$ mJ mol^{-1} K^{-2}, which is nearly one-third of the value for MgCNi$_3$.[5]

We plotted the same specific-heat data in an alternative form C_p/T versus T in the inset of Fig. 5. The plot allows us
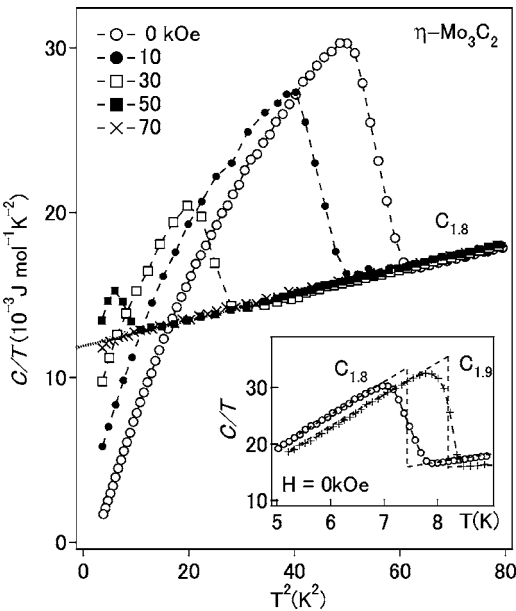
FIG. 5. Characterization of the superconducting transition of the molybdenum carbide (nominal composition Mo$_3$C$_{1.8}$) by measurement of the specific heat under a variety of magnetic field. (Inset) C/T vs T plots to determine a change in the specific heat at the superconducting transition.
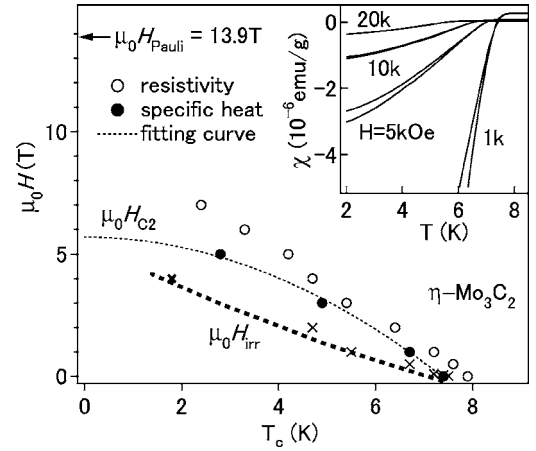
FIG. 6. Upper critical field determined from the resistivity (open circles) and the specific heat (closed circles) measurements. The fine dotted curve is a fit to the data (see text). Inset shows represents of magnetic susceptibility curves to determine the irreversible point between the ZFC and the FC curves. The irreversibility points found out in the way are plotted in the main panel as fine crosses. The fat cross indicated the point determined by the magnetization study at 1.8 K [Fig. 3(b)]. The fat dotted line is a guide to eyes. Pauli's limit is indicated by an arrow.

to determine the midpoint of the thermodynamic transition, as well as the jump $\Delta C/T_c$. The transition midpoint is 7.4 K (for the sample with the nominal composition Mo$_3$C$_{1.8}$), which is slightly below the resistivity onset. The midpoint for the sample with the nominal composition Mo$_3$C$_{1.9}$ is 8.2 K, giving us clear evidence that the superconducting transition depends on the charge-carrier concentration. A quantitative estimation of the charge carrier is left for future work. We found $\Delta C/T_c$ is 17.5 mJ mol^{-1} K^{-2} and 19.8 mJ mol^{-1} K^{-2} for the C$_{1.8}$ and the C$_{1.9}$ samples, respectively. The values lead the factor $\Delta C/\gamma T_c$ to 1.48 for the C$_{1.8}$ sample, which is nearly identical with the BCS value of 1.43 for a weakly coupled superconductor.[16]

The upper critical field of η-Mo$_3$C$_2$ (nominal composition Mo$_3$C$_{1.8}$) determined by the resistivity and the specific-heat measurements are shown in Fig. 6. A 1% screening was applied to find out the onset of the resistivity transition under the magnetic field (Fig. 4).[17] The resistivity data points are slightly above the specific-heat ones, suggesting a small carbon stoichiometry variation in the sample, in consistent with the results of the neutron diffraction analysis. Hence, we employed the specific-heat data to determine the upper critical field because those seem to reflect an average of the variation.

The upper critical filed at $T=0$ was estimated by an extrapolation method using a conventional formula $H_{C2}(T) = H_{C2}(0)[1-(T/T_C)^2]$ for a weakly coupled superconductor.[11] A least-squares fit to the data yielded $\mu_0 H_{c2}(0) = 5.7(2)$ T, as shown in Fig. 6. Alternatively, we tested another formula $\mu_0 H_{c2} = -0.693(dH_{c2}/dT)_{T=T_c} T_c$ developed within the weak-coupling BCS theory by Werthamer *et al.*[18] As a result, we obtained $\mu_0 H_{c2(0)} = 5.6(1)$ T, which is in a good agreement with the other result. Meanwhile, the Pauli-limiting field was calculated to be 13.9 T in regards to $\mu_0 H_{Pauli} = 1.24 k_B T_c/\mu_B$,

where $T_c = 7.4$ (the midpoint of the specific-heat jump). The value of $\mu_0 H_{Pauli}$ is larger than double of $\mu_0 H_{c2}(0)$, suggesting a pair-breaking effect due to the Zeeman energy is substantial in η-Mo_3C_2.

The evaluation of $H_{c2}(0)$ then allows us to estimate the coherence length ξ at $T = 0$ using the formula $\xi(0) = \sqrt{\Phi_0 / 2\pi H_{c2}(0)}$ (where Φ_0 is the flux quantum), being valid for a weakly coupled superconductor.[16] The value $\xi(0) = 7.6$ nm was obtained. It is approximately 70% longer than that of $MgCNi_3$ and $\sim 20\%$ shorter than that of Li_2Pd_3B. We discuss the issue later.

The magnetic irreversible feature was studied by a magnetic susceptibility method. Representative susceptibility curves measured in intense magnetic fields are shown in the inset of Fig. 6. The same criterion used in the M versus H study [shown in Fig. 3(b)] was employed and the determinations are plotted in the main panel as crosses. The irreversible area in the superconducting diagram is slightly larger than that for the structurally isotropic compound Li_2Pd_3B which has nearly the same T_c,[19–22] reflecting possible enhancement of vortex liquid or glass states due to the enhanced anisotropic feature of η-Mo_3C_2.[23] To deepen understanding of the superconducting dimensionality of η-Mo_3C_2, a single-crystal study would play a pivotal role if it is available.

The lower critical field was measured by a magnetic susceptibility method using a conventional formula $H_{C1}(T) = H_{C1}(0)[1 - (T/T_C)^2]$ for a weakly coupled superconductor.[16] The original data show a magnetization characteristic in the vicinity of the lower critical field, and it is shown with the main panel of Fig. 7. In our analysis, the minimum point of the data curve was employed as the lower critical field at each temperature, and $\mu_0 H_{c1}(T)$ was plotted in the small panel of Fig. 7. A least-squares fitting to the points using the formula yielded $\mu_0 H_{c1}(0) = 0.0138(2)$ T, which is comparable with the values reported for Li_2Pd_3B (0.0135 T) (Refs. 19–22) and $MgCNi_3$ (0.01 T).[24–26] The $\mu_0 H_{c1}(0)$ estimation then allows us to evaluate the magnetic penetration depth (λ), as the lower critical field is associated with λ and ξ through the relation $H_{C1}(T) = (\Phi_0 / 4\pi\lambda^2)\ln(\lambda/\xi)$. The value $\lambda(0) = 197$ nm was obtained.
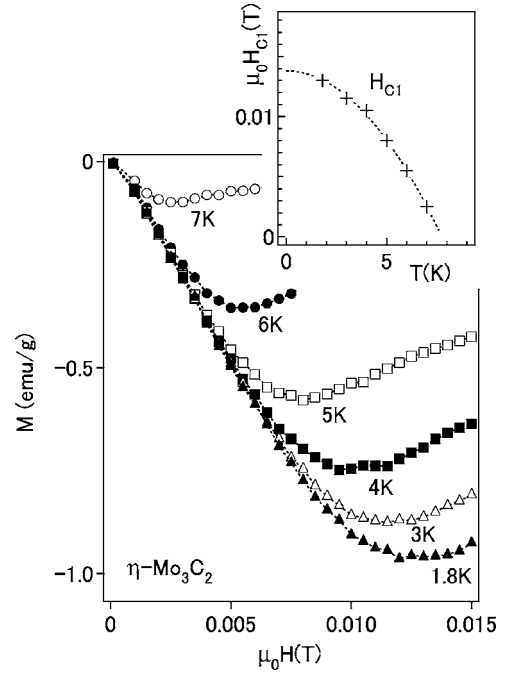
FIG. 7. Lower critical field determined from the magnetization measurements. The dotted curve in the top panel is a fit to the data.

The Ginzburg-Landau parameter $\kappa (\equiv \lambda/\xi)$ was then calculated to be 26. It is comparable with that for Li_2Pd_3B (~ 21),[22] but less than a half of that for $MgCNi_3$ (~ 54).[25] The thermodynamical critical field $H_c(0)$ was also estimated through the relation $H_C(0) = \sqrt{H_{c1}(0)H_{c2}(0)/(\ln\kappa + 0.08)}$, which is valid for $\kappa \gg 1$.[16] The estimation resulted in $\mu_0 H_c(0) = 0.15$ T.

IV. CONCLUSIONS

In summary, the superconducting parameters of η-Mo_3C_2 were measured and compared with those of the related compounds Li_2Pd_3B and $MgCNi_3$, which have comparable T_c and share the common structure basis, comprising six-hold carbons (borons) by transition metals. The super-

TABLE II. Comparison of superconducting parameters of η-Mo_3C_2 with related compounds.

Parameters	Unit	η-Mo_3C_2	Li_2Pd_3B (Refs. 20–23)	$MgCNi_3$ (Refs. 25–27)
T_c	K	7.4	7.5	7.6
$\mu_0 H_{C1}(0)$	T	0.014	0.014	0.010
$\mu_0 H_C(0)$	T	0.15	0.15[a]	0.19
$\mu_0 H_{C2}(0)$	T	5.7	4.8	14.4
$\lambda(0)$	nm	197	194	248
$\xi(0)$	nm	7.6	9.1	4.6
$\kappa(0)$		26	21	54
γ	mJmol^{-1} K^{-2}	11.8	9.0	30.1
$\Delta C / \gamma T_C$		1.48	2.0	2.1

[a]Calculated by the same method in this study using the reported values of $\mu_0 H_{C1}(0)$, $\mu_0 H_{C2}(0)$, and $\kappa(0)$ for Li_2Pd_3B.

conducting parameters of those are listed in Table II. The comparison indicates that the superconducting properties of η-Mo$_3$C$_2$ are rather comparable with those of the boride superconductor and are not with the carbon-based one. At this moment, we are unable to explain reasons for the similarities and the differences over these superconducting properties; however, one possibility the present results indicate is that the unusual mechanism of the superconductivity is likely for MgCNi$_3$,[5] because the coherence length of MgCNi$_3$ is shorter than those of others. The short coherence could be a possible indication of unconventional superconductivity, as intensively discussed in theoretical works.[27–30] The lager $\kappa(0)$ of MgCNi$_3$ than the others also indicates the same possibility.

Although the structure character of η-Mo$_3$C$_2$ was found to be rather anisotropic due to the preferred carbon vacancies at the C2 site, we did not see any clear evidence of possible superconducting anisotropy. Perhaps a careful investigation into a single crystal of η-Mo$_3$C$_2$ could be a promised way to verify the possibility if it becomes available.

Within our investigation, we were unable to determine whether the mechanism of the superconductivity of η -Mo$_3$C$_2$ was understandable within the weak-coupling BCS model. Further evaluations of the superconducting dimensionality, a role of the Mo $4d$ bands with respect to the $4d$ magnetism, the mean-free path, and the density of charge carriers responsible for the superconductivity are at least needed to reach a strong conclusion.

ACKNOWLEDGMENTS

*Author to whom correspondence should be addressed. Fax. +81-29-860-4674. Email address: YAMAURA.Kazunari@nims.go.jp

[1] H. J. Choi, D. Roundy, H. Sun, M. L. Cohen, and S. G. Louie, Nature **418**, 758 (2002).

[2] R. J. Cava, H. W. Zandbergen, B. Batlogg, H. Eisaki, H. Takagi, J. J. Krajewski, W. F. Peck, E. M. Gyorgy, and S. Uchida, Nature **372**, 245 (1994).

[3] R. J. Cava, H. Takagi, B. Batlogg, H. W. Zandbergen, J. J. Krajewski, W. F. Peck, R. B. Vandover, R. J. Felder, T. Siegrist, K. Mizuhashi, J. O. Lee, H. Eisaki, S. A. Carter, and S. Uchida, Nature **367**, 146 (1994).

[4] R. J. Cava, H. Takagi, H. W. Zandbergen, J. J. Krajewski, W. F. Peck, T. Siegrist, B. Batlogg, R. B. Vandover, R. J. Felder, K. Mizuhashi, J. O. Lee, H. Eisaki, and S. Uchida, Nature **367**, 252 (1994).

[5] T. He, Q. Huang, A. P. Ramirez, Y. Wang, K. A. Regan, N. Rogado, M. A. Hayward, M. K. Haas, J. S. Slusky, K. Inumara, H. W. Zandbergen, N. P. Ong, and R. J. Cava, Nature **411**, 54 (2001).

[6] N. S. Athanasiou, Mod. Phys. Lett. B **11**, 939 (1997).

[7] B. V. Khaenko, T. Ya. Velikanova, and V. Z. Kublii, Inorg. Mater. **23**, 365 (1987).

[8] V. Z. Kresin, Phys. Lett. A **122**, 434 (1987).

[9] V. Z. Kresin and V. P. Parkhomenko, Sov. Phys. Solid State **16**, 2180 (1975).

[10] R. H. Willens and E. Buehler, Appl. Phys. Lett. **7**, 25 (1965).

[11] L. E. Toth, E. Rudy, J. Johnston, and R. Parker, J. Phys. Chem. Solids **26**, 517 (1965).

[12] E. V. Clougherty, K. H. Lothrop, and J. A. Kafalas, Nature **191**, 1194 (1961).

[13] http://www.ncnr.nist.gov/

[14] B. H. Toby, J. Appl. Crystallogr. **34**, 210 (2001).

[15] A. C. Larson and R. B. Von Dreele, Los Alamos National Laboratory Report No. LAUR 86–748, 2004, unpublished.

[16] J. P. Carbotte, Rev. Mod. Phys. **62**, 1027 (1990).

[17] R. H. T. Wilke, S. L. Bud'ko, P. C. Canfield, J. Farmer, and S. T. Hannahs, Phys. Rev. B **73**, 134512 (2006).

[18] N. R. Werthamer, E. Helfand, and P. C. Hohemberg, Phys. Rev. **147**, 295 (1966).

[19] H. Takeya, K. Hirata, K. Yamaura, K. Togano, M. El Massalami, R. Rapp, F. A. Chaves, and B. Ouladdiaf, Phys. Rev. B **72**, 104506 (2005).

[20] H. Takeya, K. Yamada, K. Yamaura, T. Mochiku, H. Fujii, T. Furubayashi, K. Hirata, and K. Togano, Physica C **426-431**, 411 (2005).

[21] K. Togano, P. Badica, Y. Nakamori, S. Orimo, H. Takeya, and K. Hirata, Phys. Rev. Lett. **93**, 247004 (2004).

[22] P. Badica, T. Kondo, T. Kubo, N. Nakayama, S. Orimo, and K. Togano, Appl. Phys. Lett. **85**, 4433 (2004).

[23] Y. Yeshurun, A. P. Malozemoff, and A. Shaulov, Rev. Mod. Phys. **68**, 911 (1996).

[24] X. F. Lu, L. Shan, Z. Wang, H. Gao, Z. A. Ren, G. C. Che, and H. H. Wen, Phys. Rev. B **71**, 174511 (2005).

[25] Z. Q. Mao, M. M. Rosario, K. D. Nelson, K. Wu, I. G. Deac, P. Schiffer, Y. Liu, T. He, K. A. Regan, and R. J. Cava, Phys. Rev. B **67**, 094502 (2003).

[26] S. Y. Li, R. Fan, X. H. Chen, C. H. Wang, W. Q. Mo, K. Q. Ruan, Y. M. Xiong, X. G. Luo, H. T. Zhang, L. Li, Z. Sun, and L. Z. Cao, Phys. Rev. B **64**, 132505 (2001).

[27] S. Stintzing and W. Zwerger, Phys. Rev. B **56**, 9004 (1997).

[28] N. Trivedi and M. Randeria, Phys. Rev. Lett. **75**, 312 (1995).

[29] P. A. Lee, Phys. Rev. Lett. **71**, 1887 (1993).

[30] M. Randeria, N. Trivedi, A. Moreo, and R. T. Scalettar, Phys. Rev. Lett. **69**, 2001 (1992).